Design and Evaluation of an IMU Sensor-based System for the Rehabilitation of Upper Limb Motor Dysfunction

Bao Tran, Xiaorong Zhang, Amir Modan, and Charmayne M.L. Hughes

***Abstract*— Stroke is one of the most significant non-communicable diseases in the world with approximately 15 million people experiencing a new or recurrent stroke each year. Nearly half of stroke survivors have some degree of permanent sensorimotor impairment and require specialized rehabilitation. Wearable technologies are a cost-effective means by which to monitor and provide feedback about sensorimotor function across the different phases of stroke recovery, with insights improving decision-making by rehabilitation clinicians and increasing accountability and motivation for the patient. In this paper, we design and evaluate a wearable sensor system that measures movement kinematics during the performance of activities of daily living. Results indicate high to very high agreement and correlation values between the sensor and the gold-standard motion capture system, regardless of kinematic parameter. In sum, the described sensor is capable of accurately measuring upper limb movement kinematics, using only a single sensor. The adoption of portable and low-cost devices have the ability to make a substantial impact for the millions of persons who exhibit motor impairments after a stroke.**

I. Introduction

Stroke is the leading cause of disability in the United States, with 65% of the nearly four million people who have survived a stroke living with minor to severe impairments [1]. Individuals are left with a broad range of disabilities, from mild paresis to complete paralysis of both the upper and lower limbs, proprioceptive deficits, disordered movement organization, loss of range of motion, muscle weakness and abnormal muscle tone, and impaired force generation. Impaired arm and hand function significantly contributes to limitations in the ability to perform activities of daily living (ADLs), and has a detrimental effect on patients' capacity for independent living and economic self-sufficiency [2].

The primary goal of stroke rehabilitation is to motor function, maximize functional independence, and improve quality of life. Conventional rehabilitation strategies incorporate repetitive motor or task practice to facilitate neuroplasticity and brain reorganization, resulting in enhanced functional motor recovery [3]. However, this mode of rehabilitation requires frequent one-on-one interactions with therapists that can last for several months, and place a significant burden on rural and remote communities struggling with a shortage of physical rehabilitation health professionals crucial to the delivery of services [4]. Individuals residing in remote and rural locations have to travel long distances to access the same services that urban residents can more easily access, which places a substantial burden on patients living in these communities, especially for individuals with low incomes, no paid time off from their jobs, physical limitations, or without access to personal transportation. he systemic barriers that rural and remote residents face when accessing rehabilitation services can be addressed through the development of technology-enabled solutions, allowing rural patients to see specialists in a timely manner from the comfort of their home, while also considering the extant barriers to healthcare access and infrastructure that rural communities face.

The bulk of this work has focused on developing and deploying motion analysis systems [5-6] and robotic systems [7-8], both of which exhibiting better diagnostic and prognostic precision, and are more likely to discriminate subtle differences of deficit and changes over time, than current clinical measures. For example, [5] used a five camera Qualisys motion capture system to example movement kinematics during a multi-step ADL in stroke patients and healthy control participants, and found that stroke patients took longer to complete the task, and exhibited lower mean peak velocity values than age-matched control participants. Thus, while there are many benefits to using motion capture and robotic systems, their high costs, bulk, and technical knowledge requirements limit their application to rural communities and decentralized environments (i.e., community centers or patient's home).

As such, a number of research groups have capitalized on developments in inertial measurement unit (IMU) hardware technology and signal processing techniques that can adequately correct sensor bias and dynamic drift [9], and investigated whether these devices are capable of providing the level of accuracy and validity required for post-stroke motor assessment [10-13]. In addition to their low cost, portability, and unobtrusiveness, there is evidence that IMU systems can provide precise quantitative kinematic measurements that enable clinicians to identify pathological movement, characterize disease state, and track recovery progress [11, 13]. For example, our research group has developed a low-cost rehabilitation system that uses a single IMU and advanced signal-processing algorithms to record upper limb movements and derive metrics that are meaningful to both clinicians and patients [10-11]. The validity of the sensor was recently compared to a gold standard optoelectronic motion capture system [10], with results indicating strong positive correlations and agreement with the reference system, regardless of task or kinematic parameter. The sensitivity of the sensor was then tested in patients with acquired brain injury (i.e., stroke, traumatic brain injury) [11], with results demonstrating that the sensor is capable of discriminating between different arm impairment levels and the hand performing the task (unimpaired, impaired).

While the sensor system proved to be a useful tool in the evaluation of sensorimotor dysfunction, the system consisted

*This project was partially supported by the United States National Science Foundation (NSF #2139697 and NSF #1752255).

Bao Tran, Xiaorong Zhang, and Amir Modan are with the School of Engineering at San Francisco State University, San Francisco, CA 94132 USA. (e-mail: btran12@mail.sfsu.edu).

C.M.L. Hughes is with the Health Equity Institute, San Francisco, CA 94132 USA (415-405-2540; e-mail: cmhughes@sfsu.edu).

of cumbersome breakout modules and a portable battery bank which yielded a total volume of 242,748 mm^3 and weight of 450 g (Fig 1A). As such, while upper limb movement kinematics could be accurately measured using the sensor, substantial changes needed to be made to improve the weight and robustness of the system before initiating clinical trials in decentralized locations.

As such, the aim of the present study was to redesign the system into a single printed circuit board (PCB) and lithium-ion (li-ion) battery. In doing so, a more lightweight and robust sensor system (hereafter referred to as the T'ena sensor) can be deployed to decentralized environments, such as community centers or patients' homes. To address this question, participants performed an object manipulation task taken from the Action Research Arm Test (ARAT) [14], and data collected by the T'ena sensor was compared to simultaneously recorded measures from a gold-standard optoelectric motion capture system (Vicon motion capture system). Results of this study will provide a better understanding of the validity and reliability of a single IMU-based sensor system for accurately measuring movement kinematics.

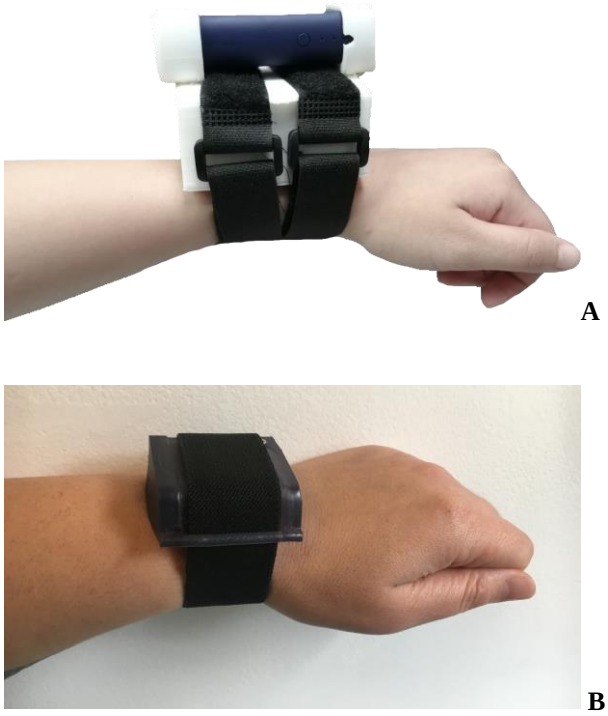

Fig. 1. Original sensor (A: top) and redesigned T'ena sensor (B: bottom) placed on a participant's wrist

II. METHODS

A. *Hardware and Firmware Design of the T'ena Sensor*

1) *Original Design*

The original IMU sensor prototype (Fig. 1A) was composed of a Tiva C Series TM4C123G microcontroller LaunchPad, a GY-91 MPU-9250 sensor breakout, an HC-05 Bluetooth breakout, and a portable USB power bank. The three breakout boards were encased in a 3D printed polylactic acid (PLA) filament encloser (83H x 59W x 39D mm) while the battery bank (29H x 21W x 85D mm) was attached to the top of the enclosure. The sensor system was attached to the wrist using Velcro straps. For the firmware design, the microcontroller reads raw accelerometer and gyroscope data from the GY-91 sensor using an Inter-Integrated Circuit (I^2C) interface and transmits data to the HC-05 Bluetooth module via the Universal Asynchronous Receiver-Transmitter (UART) interface whenever a new data sample is collected. More details about the original sensor design can be found in [10].

2) *Design of the T'ena Sensor*

The new T'ena sensor system (Fig. 1B) consists of three main components, an ESP32-WROOM32D microcontroller module (Espressif), an ICM20689 IMU sensor (Invensense), and a 400mAh li-ion battery (Sparkfun). The ESP32-WROOM32D module was chosen for its low cost (single unit cost of $6.825), small size, and its integration of an on-board Bluetooth module. The ICM20689 IMU sensor was selected because of its low cost (single unit cost of $6.09) and its similarity to the original MPU-9250 IMU sensor, which is now an end-of-life product. A custom PCB (Fig. 2) was designed to minimize space and reduce connection fragility, which was an issue with the original sensor due to the use of separate breakout boards. A USB-C connector was integrated into the system and custom circuits were developed to charge, program, and monitor the sensor via USB. Finally, powering on the PCB is controlled by an easy-to-use touch-on-hold-off push button circuit.

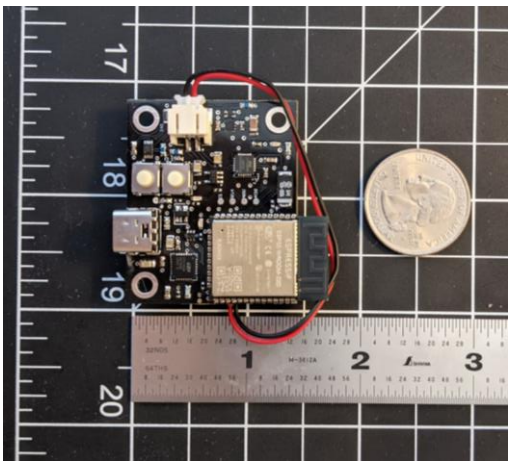

Fig. 2. Redesigned sensor with the ESP32-WROOM32D module, ICM20689 IMU sensor, and 400mAh li-ion battery (not visible).

The enclosure was designed using stereolithographic (SLA) 3D printing, which uses a laser to cure liquid resin into hardened plastic. SLA build lines have a thickness of 0.05 mm, whereas PLA plastic parts have a build thickness of 0.25 mm. As such, SLA resin parts have five times the layer resolution of acrylonitrile butadiene styrene (ABS) plastic parts, which yield crisper and higher-resolution detail.

In sum, the redesigned sensor system weighed 60 g with a total size of 50H x 70W x 20D mm (total volume of 70,000 mm^3). Thus, the weight of the sensor was reduced by 390 g and the total size by 172,748 mm^3. The firmware of the sensor has also been improved by replacing the I^2C-based data collection module with a new module that integrates the Serial Peripheral Interface (SPI) and a First-In-First-Out (FIFO)

buffer to achieve higher efficiency and timing precision with processing and transmission of bulk measurements.

B. Participants

Ten participants from the San Francisco State University campus (mean age = 38.2, SD = 14.9) participated in the present study. Based on administration of the Revised Edinburgh Handedness Inventory [15] which ranks handedness in a battery of common tasks on a scale ranging from −1 (strongly left-handed) to 1 (strongly right-handed), all participants were right handed (mean = 93.61, SD = 6.73). The study was approved by the San Francisco State University Institutional Review Board committee.

C. Tested Systems

Accelerometer and gyroscope data was collected from the T'ena sensor. Initial calibration of the IMU occurs at the start of each data collection session, and consisted of placing the sensor on a flat table until 1,000 data points were captured. During each trial, the raw data were sent from the IMU to the microcontroller via the SPI communication protocol, and then to a custom application on a personal computer via classic Bluetooth which saved the incoming data stream in a CSV file for later off-line processing.

Criterion reference kinematic data was collected using an eight camera Vicon motion capture system (Bonita 10, VICON Motion Systems), with a temporal and spatial resolution of 100 Hz and 1 mm, respectively. One 9.5 mm reflective markers was attached to the T'ena sensor and used to calculate movement kinematics during task performance.

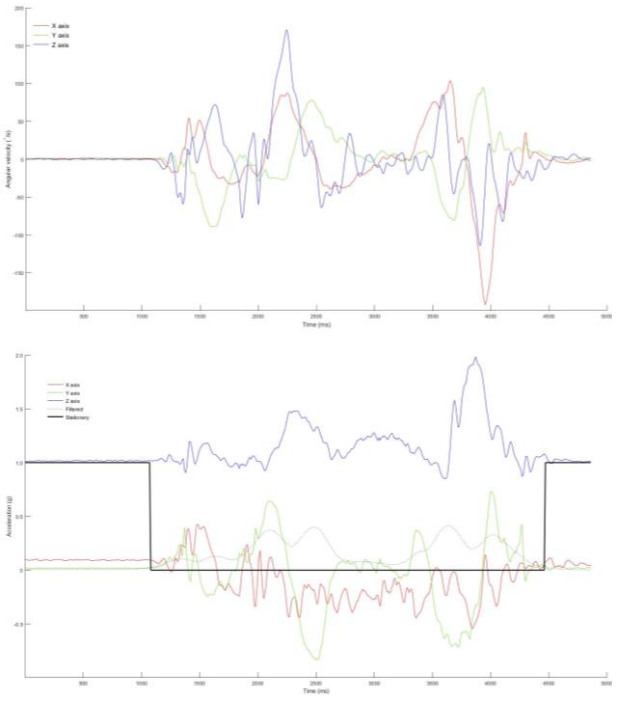

Fig. 3. Representative raw data from the gyroscope (top panel) and accelerometer (bottom panel). The relevant gesture is separated from stationary periods at the beginning and end of the data capture.

C. Procedure

After reading and filling out the written informed consent forms, the participant sat upright in a chair with a firm back and no armrests. The sensor was then placed on the dominant hand, and they placed their hand on the starting position located on the table in a pronated orientation. Upon the verbal signal from the experimenter, the participant performed the Block Task from the grasp subtest of the Action Research Arm Test (ARAT) [14]. In this task, the participant grasped a 5 cm^3 block from the table, placed it on the top of a 37 cm high shelf placed 25 cm away from the proximal edge of the table, and then bought their hand back to rest on the starting position. Participants were instructed to perform the task at a comfortable speed, and to grasp the object in such a way that it would not slip during the fingers during transportation.

D. Data Processing

The 3D coordinates of the Vicon marker were reconstructed and labeled for each individual trial, filtered using a Woltring filter with a predicted mean square error value of 5 mm Vicon Nexus 2.2) and exported in CSV format. Using a custom written MATLAB (The MathWorks®, Version R2021a) script, the 3D position data of each axis was transformed into movement velocity using a first-order central difference technique, and then the individual vector velocities were summed to derive resultant velocity.

The raw gyroscope and accelerometer values obtained from the T'ena sensor were offline processed by a custom program written in MATLAB (The MathWorks, Version R2021a). While more details can be found in [10], the data sets were trimmed based on a stationary detection threshold to exclude stationary sections at the beginning and end of the recorded gesture (Figure 3). An Attitude Heading Reference System (AHRS) filter was used to compute the current IMU orientation and transform data from the local sensor frame to the global earth frame. Additionally, 1 g was subtracted from the z-axis acceleration to account for gravitational acceleration effects. Subsequently, the integral of the acceleration signal was calculated to derive velocity separately for the three axes. Resultant velocity was then calculated by summing the individual vector velocities.

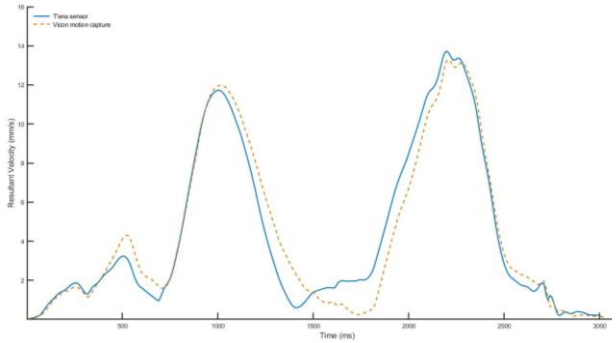

Fig. 4. Representative resultant velocity trajectory for the T'ena sensor (solid blue lines) and the Vicon motion capture system (dashed orange lines).

For each Vicon and T'ena sensor trial, data analysis was restricted to the time period between when the hand left the starting position (movement onset) to the time the hand returned to the starting position (movement offset). Based on prior literature [10-11], as well as more recent pilot testing, it was expected that the resultant velocity profile would exhibit three peaks for this particular ADL task. As such, movement onset and offset were determined using kinematic criterion. Specifically, movement onset was determined as the instant when resultant velocity exceeded 1.5% of the first velocity peak. Movement offset was determined as the moment when the velocity trace dropped, and remained, below 1.5% of the last peak.

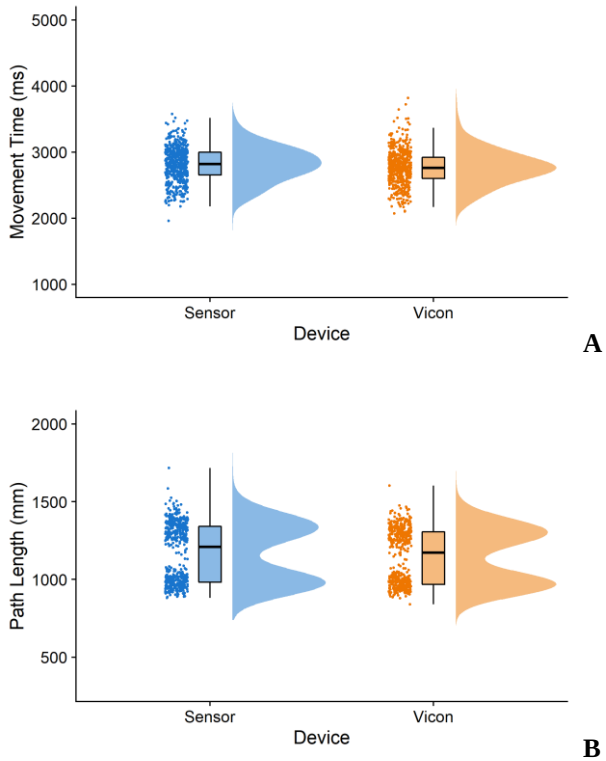

Fig. 5. Raincloud plots showing the data distribution, and five summary statistics for the T'ena sensor (dark grey) and the Vicon motion capture system (light grey) for A) Movement time and B) Path Length.

E. Statistical Analysis

Four kinematic variables were derived based on their sensitivity to detect differences in motor dysfunction and use in clinical settings [16]: Total movement time (ms), Path Length (mm), Peak Velocity of the Placing Phase (mm/s), and Peak Velocity of the Return Phase (mm/s). Total movement time is defined as the time period from movement onset to movement offset. Path Length is defined the total displacement of the hand from the beginning to the end of the movement. The Block task can be divided into a placing phase and a return phase. The placing phase was defined as the time period between when the block was lifted from the table to the time the block contacted the shelf top. The return phase was defined as the time period between when the object contacted the shelf top to when the hand was placed on the back on the table. For these two phases, peak velocity was calculated by determining the maximal resultant speed reached in the given phase.

To validate the ability of the T'ena sensor to measure upper limb kinematics, Pearson product moment correlation coefficients (*r*) were calculated to quantify the degree to which the T'ena sensor and the gold standard Vicon motion capture system are related. Rowntree's [17] conventions were used to interpret coefficients, with values < 0.20 classified as very weak, values between 0.20 – 0.40 classified as weak, values between 0.40 – 0.70 classified as moderate, values between 0.70 - 0.90 as strong/high, and values > 0.90 as very strong/very high. Additionally, intra class correlation coefficients (ICC2,1) were used to evaluate inter-sensor reliability, using the absolute agreement definition between the original and redesigned system [18]. The strength of the relationship was determined using Evans [19] empirical classifications in which values lower than 0.20 are considered as very weak, values between 0.20 - 0.39 are considered weak, values between 0.40 – 0.59 are considered moderate, values between 0.60 – 0.79 are considered strong, and values between 0.80 - 1.0 are considered very strong.

III. RESULTS

Overall, 596 trials where obtained with both the T'ena sensor and an 8-camera Vicon motion capture system. As can be seen in Fig. 4, the T'ena sensor produced resultant velocity trajectories representative of the Block Task [10-11], with kinematics that were similar to that captured by the gold-standard Vicon motion capture system.

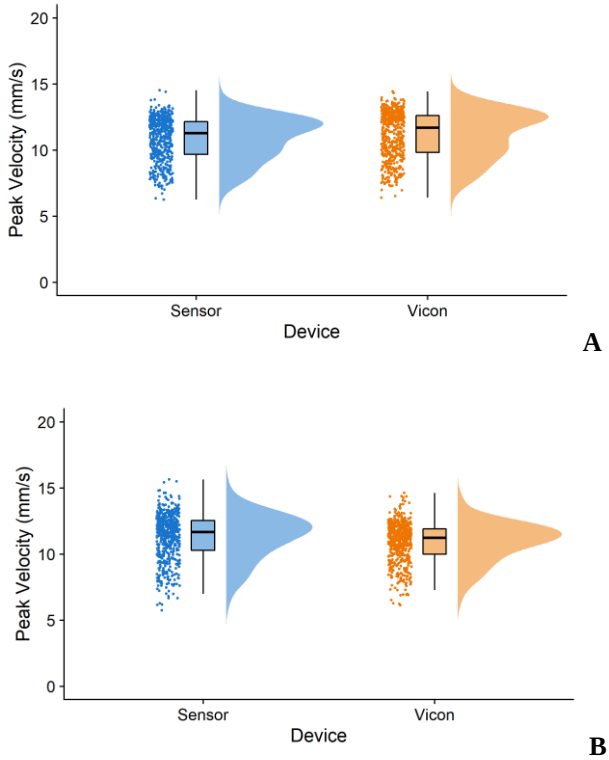

Fig. 6. Raincloud plots showing the data distribution, and five summary statistics for the T'ena sensor (dark grey) and the Vicon motion capture system (light grey) for A) Peak Velocity of the Placing Phase, and B) Peak Velocity of the Return Phase.

Raincloud plots that depict the data distribution and summary statistics (i.e., median, first quartile, third quartile, minimum, and maximum) are shown in Fig 5 (movement time, path length) and Fig 6 (peak velocity of the placing phase, peak velocity of the return phase). In general, the data was normally distributed for the movement time and return phase peak velocity, whereas peak velocity of the placing phase, was positively skewed, and path length exhibited a bimodal distribution. Despite these differences due to kinematic parameter, the shape of the distribution (as well as the five summary statistics values) were similar for both the T'ena sensor and Vicon system.

Examining the relationship and absolute agreement between the sensors, it was clear that there was a very high level of agreement for all metrics (Figure 7). Pearson product moment correlation values were strong/high for the movement time variable (r = 0.720), and very strong/very high for path length r = 0.962, peak velocity of the placing phase (r = 0.939), and peak velocity of the return phase (r = 0.917), all p's < 0.05. Intra class correlation coefficients showed a similar pattern of results, with the level of absolute agreement between the two systems classified as strong for the movement time metric (ICC = 0.706), and very strong for the path length (ICC = 0.952), peak velocity of the placing phase (ICC = 0.920), and peak velocity of the return phase (ICC = 0.878).

IV. DISCUSSION

Conventional physical therapy is a time and labor-intensive process that is plagued by low patient engagement, satisfaction, and adherence. Current technology-based solutions involve optoelectric motion capture systems that record 3D position of reflective markers and actuated robotic devices that generate driving forces to help the patient move through space [5-8]. Despite their high accuracy, many of these systems have not been commercially successful because of their high cost, safety issues, and bulkiness that limit their application to decentralized environments (i.e., community centers or patient's home). As such, the aim of the present study was to determine the ability of the T'ena IMU sensor-based system to reliably and accurately assess movement quality and efficiency in physically and neurologically healthy adults.

Statistical analysis indicated high to very high correlations (r range = 0.720 – 0.962) and absolute agreement values (ICC range = 0.706 – 0.952) between the T'ena sensor and reference system, regardless of kinematic metric. Of the four measured kinematic metrics, correlations and absolute agreement values were the lowest for the movement time metric. This is most likely due to the fact that the IMU is less sensitive to the very low movements that occur at the start and end of the movement. To correct for this issue, future work will involve exploring whether parameter tuning of the stationary detection threshold and/or AHRS filter algorithms can improve the accuracy of the T'ena sensor to detect movement onset and offset. Additionally, we will explore whether deep learning algorithms (e.g., convolutional neural networks) [20] are better able to improve the accuracy of the T'ena sensor by learning the non-dimensional relationship from the high-dimensional data collected by the T'ena sensor and a reference system.

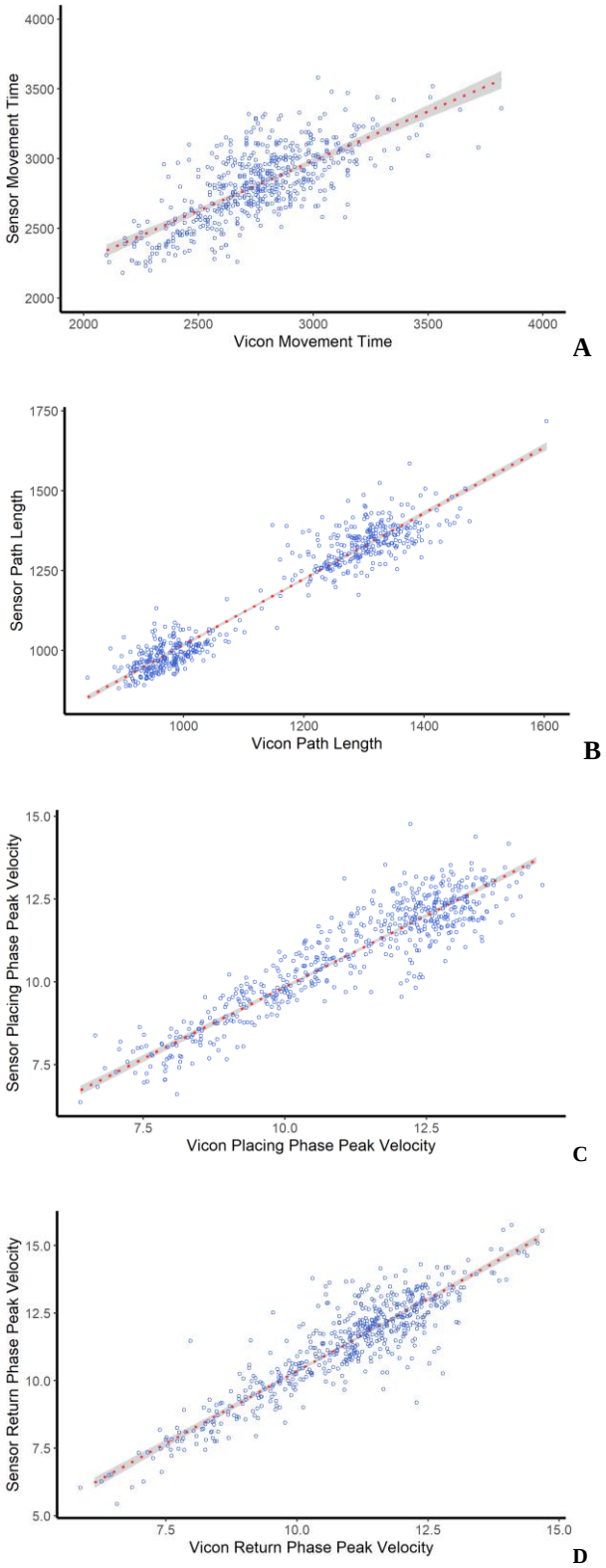

Fig. 7. Correlation plots between the T'ena sensor and Vicon. A) Movement time, B) Path Length, C) Peak Velocity of the Placing Phase, and D) Peak Velocity of the Return Phase

Some of the limitations of the study include the evaluation of a single post-stroke upper limb ADL, and measuring performance in only neurologically healthy individuals. In future studies, we will determine the ability of the T'ena sensor to measure a variety of ADL tasks associated with motor impairment and disability scales, such as the Motor Assessment Scale (MAS), the Melbourne Assessment of Unilateral Upper Limb Function, and the Fugl-Meyer Upper Extremity Motor Assessment [uFMA]). In addition, motor performance will be measured in a heterogenous sample of post-stroke individuals, with sensor metrics compared with values obtained from clinical scales. This work will enable us to determine the tasks, as well as the level of motor impairment, that the T'ena sensor is capable of accurately measuring.

From a technical and commercialization perspective, performance metrics (e.g., processing delay, communication latency, data loss rate, memory and power consumption) will be measured, after which extensive analysis will be done to evaluate relations and trade-offs between these performance metrics in order to identify optimal settings for the system. Concurrently, the T'ena sensor will be integrated into the T'ena rehabilitation mobile application [21], after which the ability of the system to support recovery for individuals with stroke in their home environment will be examined.

Despite these limitations, the results of the study are promising and indicate the potential to use the redesigned sensor for decentralized rehabilitation. The research described in this paper is innovative because it proposes a new home-based approach to physical and neurological rehabilitation management, which up until now has been conducted in clinics. The long term goal of this work is to leverage mobile and wearable technologies to address the primary reasons why patients do not remain compliant with their plan of care – access and convenience. By facilitating successful establishment of technology-enabled home-based rehabilitation of persons with motor impairments, the T'ena system could lead to a paradigm shift in the way that neurological disorders and physical injuries are managed, and would lead to improvements in clinical practice and access to care in medically underserved areas (e.g., health professional shortage areas [HPSAs] and medically underserved areas [MUAs]) or during situations where in-person medical care is contraindicated (e.g., the COVID-19 pandemic).

REFERENCES

[1] A. S. Go *et al*., "Heart disease and stroke statistics—2014 update: a report from the American Heart Association", *Circulation*, vol. 129, no. 3, Dec. 2013, doi: 10.1161/01.cir.0000441139.02102.80.

[2] B. Bates *et al*., "Veterans affairs/department of defense clinical practice guideline for the management of adult stroke rehabilitation care executive summary", *Stroke*, vol. 36, no. 9, pp. 2049–2056, Sep. 2005, doi: 10.1161/01.STR.0000180432.73724.AD.

[3] L. Carey *et al*., "Finding the intersection of neuroplasticity, stroke recovery, and learning: scope and contributions to stroke rehabilitation". *Neural Plast*, 2019.

[4] C. O. B. Cherry *et al*., "Expanding stroke telerehabilitation services to rural veterans: a qualitative study on patient experiences using the robotic stroke therapy delivery and monitoring system program", *Disabil Rehabilitation Assist*, vol. 12, no. 1, pp. 21-27, 2015, doi: 10.3109/17483107.2015.1061613.

[5] P. Gulde, C. M. L. Hughes, and J. Hermsdörfer, "Effects of stroke on ipsilesional end-effector kinematics in a multi-step activity of daily living". *Front Hum Neurosci*, vol. 11, no. 42, 2017. DOI: 10.3389/fnhum.2017.00042.

[6] L. van Dokkum *et al*., "The contribution of kinematics in the assessment of upper limb motor recovery early after stroke". *Neurorehabil Neural Repair*, vol 28, no. 1, pp. 4-12, 2014.

[7] A. Hussain *et al*., "Self- paced reaching after stroke: A quantitative assessment of longitudinal and directional sensitivity using the H-Man planar robot for upper limb neurorehabilitation". *Front Neurosci*, no. 10, 2016. DOI:10.3389/fnins.2016.00477.

[8] F. Marini *et al*., "Robotic wrist training after stroke: Adaptive modulation of assistance in pediatric rehabilitation". *Rob Auton Syst*, vol. 91, pp. 169-178, 2017. DOI: 10.1016/j.robot.2017.01.006.

[9] L. Ricci, F. Taffoni, and D. Formica, "On the orientation error of IMU: investigating static and dynamic accuracy targeting human motion". *PLoS ONE*, vol. 11:e0161940, 2016. doi: 10.1371/journal.pone.0161940

[10] C. M. L. Hughes *et al*., "Development of a post-stroke upper limb rehabilitation wearable sensor for use in sub-Saharan Africa", *Front Bioeng Biotech*, vol. 7, Nov. 2019, doi: 10.3389/fbioe.2019.00322.

[11] C. M. L. Hughes *et al*., "Quantitative assessment of upper limb motor function in Ethiopian acquired brain injured patients using a low-cost wearable sensor", *Front Neurol*, vol. 10, Dec. 2019, doi: 10.3389/fneur.2019.01323.

[12] S. Patel *et al*., "A novel approach to monitor rehabilitation outcomes in stroke survivors using wearable technology". *Proc IEEE*, vol. 98, no. 3, pp. 450–461, 2010.

[13] A. R. Parnandi, E. Wade, M. Mataric, "Motor function assessment using wearable inertial sensors". *Conf Proc IEEE Eng Med Biol Soc*, pp. 86-89, 2010.

[14] R. C. Lyle, "A performance test for assessment of upper limb function in physical rehabilitation treatment and research", *Int. J. Ther Rehabil*, vol. 4, no. 4, pp. 483-492, 1981, doi: 10.1097/00004356-198112000-0000.

[15] M. Dragovich, "Categorization and validation of handedness using latent class analysis," *Acta Neuropsychiatr*, vol. 16, no. 4, pp. 212–218, 2004.

[16] A. Schwarz, C. M. Kanzler, O. Lambercy, A. R. Luft, and J. M. Veerbeek, "Systematic review on kinematic assessments of upper limb movements after stroke", *Stroke*, vol. 50, no. 3, pp. 718-727, 2019.

[17] Rowntree D. Statistics without Tears: A Primer for Non-Mathematicians. New York, NY: Charles Scribner's Sons; 1981.

[18] H. -Y. Kim, "Statistical notes for clinical researchers: evaluation of measurement error 1: using intraclass correlation coefficients", *Restor Dent Endod*, vol. 38, no. 2, p. 98, May 2013, doi: 10.5395/rde.2013.38.2.98.

[19] J. D. Evans, "Straightforward Statistics for the Behavioral Sciences". Pacific Grove, CA: Brooks/Cole Publishing Company, 1996.

[20] A. Arac. "Machine learning for 3D kinematic analysis of movements in neurorehabilitation", *Curr Neurol Neurosci Rep*, vol. 20, no. 8, pp. 29. DOI: 10.1007/s11910-020-01049-z.

[21] C. M. L. Hughes *et al*., "Developing an mHealth app for post-stroke upper limb rehabilitation: Feedback from U.S., and Ethiopian rehabilitation clinicians", *J Health Inform*, pp. 1-14. DOI: 10.1177/1460458219868356.